

High-spin bands in ^{80}Kr

J. Döring, V.A. Wood, J.W. Holcomb,* G.D. Johns, T.D. Johnson,† M.A. Riley,
G.N. Sylvan, P.C. Womble,‡ and S.L. Tabor

Department of Physics, Florida State University, Tallahassee, Florida 32306

(Received 1 February 1995)

High-spin states in ^{80}Kr were studied using the $^{65}\text{Cu}(^{18}\text{O},p2n)$ reaction at 65 MeV. Prompt γ - γ coincidences were measured using the Pitt-FSU detector array with nine high-purity Compton-suppressed Ge detectors and a 28-element Bismuth Germanate multiplicity filter. The previous level scheme has been extended by 16 new states up to spins and parities of 20^+ and (19^-) . The known band crossing in the positive-parity yrast band of ^{80}Kr near $\hbar\omega \approx 0.5$ MeV may be due to a $g_{9/2}$ neutron alignment, rather than a $g_{9/2}$ proton alignment as had been previously thought, based on the predicted oblate shape by Hartree-Fock-Bogolyubov calculations. No evidence was found for a second crossing in the yrast sequence up to $\hbar\omega = 0.9$ MeV. The new extension of the ground-state band through nonyrast states points to another band crossing at $\hbar\omega \approx 0.62$ MeV which may be caused by a $g_{9/2}$ proton alignment. A new negative-parity high-spin band shows that rotational bands do form at excitations above the strongly mixed low-spin levels as in the isotone ^{82}Sr .

PACS number(s): 21.10.Re, 23.20.En, 23.20.Lv, 27.50.+e

I. INTRODUCTION

The high-spin behavior of many Kr isotopes has been studied rather extensively and has provided considerable insight into the structure of f - p - g shell nuclei and the competition between single-particle and collective degrees of freedom. A rich variety of shapes, as well as shape coexistence, have been seen in the Kr isotopes, ranging from the highly deformed ^{74}Kr ($\beta_2 \approx 0.37$) [1,2] to the weakly deformed ^{82}Kr ($\beta_2 \approx 0.15$) [3]. A predicted variation of the γ deformation for low and medium-spin states ($I \leq 8\hbar$) from near-prolate in the light isotopes through triaxial to near-oblate shape in ^{80}Kr has made the question of which quasiparticle alignments are responsible for the observed band crossings in the yrast bands of the even-even isotopes more complicated than first thought. The question arises in ^{78}Kr where both triaxial and oblate shapes are predicted to coexist [4]. The triaxial shape was considered more favored until a recent g -factor discussion [5] indicated a $g_{9/2}$ neutron alignment, which should occur at the observed frequency only for an oblate shape.

The proposed $g_{9/2}$ neutron alignment in ^{78}Kr now leads to some questions about the $g_{9/2}$ proton alignment suggested for ^{80}Kr from an early cranked-shell-model analysis [6] and two-quasiparticle-plus-rotor calculations [7]. The situation is now further complicated by an ob-

served $g_{9/2}$ proton alignment in the $N = 44$ isotones ^{84}Zr [8] and ^{82}Sr [9,10], which has been confirmed by another g -factor measurement [11], and by the observation of both $g_{9/2}$ proton and $g_{9/2}$ neutron excitations at similar excitation energies in the isotope ^{82}Kr [3] and the isotone ^{78}Se [12].

Furthermore, a number of apparently mixed negative-parity states, e.g., 7^- states, was seen [6,7] in ^{80}Kr , very similar to the structure of negative-parity states in the isotone ^{82}Sr [9,10], but no negative-parity bands had been observed to higher spins. Therefore, another goal was to look for higher-lying states of negative parity connected with the onset of collectivity.

The present work was undertaken to address some of these questions about the high-spin structure of ^{80}Kr . Recent studies had been made for the lighter $^{74,76,78}\text{Kr}$ isotopes [1,2,4,13] using large γ -ray detection arrays but not for ^{80}Kr . Early investigations of the lowest members of the ground-state and the γ -vibrational bands [14–16] of ^{80}Kr were followed by rather extensive in-beam γ -ray studies at low to medium spins using α -particle induced reactions [6] and the $^{70}\text{Zn}(^{12}\text{C},2n)$ reaction [7]. In these papers the yrast positive-parity band was identified through the first band crossing up to the 6677 keV (14^+) level, and negative-parity states up to the 5158 keV (10^-) level. Recently, some low-spin states have been reinvestigated with regard to the decay of the second 0^+ state [17] at 1320.5 keV.

II. EXPERIMENTAL PROCEDURE

The fusion-evaporation reaction $^{65}\text{Cu}(^{18}\text{O},p2n)$ was used to study high-spin states in ^{80}Kr . Water, H_2^{18}O enriched to 95% in ^{18}O , was used in the Cs sputter source. The ^{18}O particles were then accelerated to 65 MeV by the

*Present address: Martin Marietta Information Systems, Mail Point 800, Orlando, FL 32825.

†Present address: Department of Physics, University of Notre Dame, Notre Dame, IN 46556.

‡Present address: Oak Ridge National Laboratory, Mail Stop 6388, Oak Ridge, TN 37830.

Florida State University Tandem-LINAC facility. The resultant beam was incident upon a thin 0.6 mg cm^{-2} self-supporting copper foil enriched to 99% in ^{65}Cu .

The Pitt-FSU detector array [18] used during this experiment consisted of nine high-purity Compton-suppressed Ge detectors, each of about 25% relative efficiency. Three Ge detectors were placed at 90° to the beam axis, two were located at 35° relative to the beam, and the remaining four detectors were positioned at 145° . A 28-element bismuth germanate (BGO) sum energy and multiplicity filter was used for part of the data acquisition as well. At least two elements of the BGO multiplicity filter had to be fired in order to accept a two or higher fold Ge detector coincidence event. Initially, a ^{152}Eu source was used for energy and efficiency calibration of all detectors. Subsequently, internal energy calibrations for the forward and backward detectors were made using the following lines: 112.0, 142.3, 238.0, and 331.4 keV from ^{76}Br ; 454.6 keV from ^{78}Kr ; 616.6 keV from ^{80}Kr ; 827.0, and 1025.9 keV from ^{79}Kr . These internal calibrations automatically correct for the Doppler shift of the γ -ray energies observed by these detectors.

A total of 1.8×10^8 prompt γ - γ coincidence events were written on 8 mm tapes. The data were sorted [19] on a DECstation 5000/200 computer, and stored as a triangular array. For every known or suspected transition in ^{80}Kr , a coincidence spectrum was projected from the array with proper background correction. These spectra were used to study the coincidence relations among the transitions in ^{80}Kr and thereby to extend the level scheme to higher spins. Three examples of background-corrected γ -ray spectra relevant for the establishment of the new high-spin levels are given in Figs. 1, 2, and 3.

To assign spins to the energy levels, directional correlation of oriented nuclei (DCO) ratios were extracted. For this purpose the data were sorted into a square array with the events from the 90° detectors on one axis and the events from the 35° and 145° detectors on the other axis. The DCO ratios were obtained by dividing the intensity

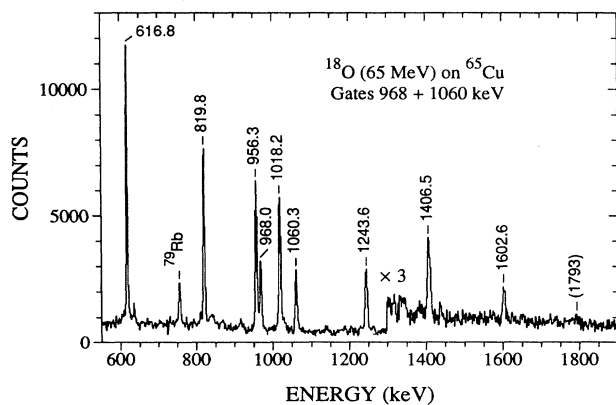


FIG. 1. Sum of spectra in coincidence with the 968 and 1060 keV transitions depopulating the 10^+ and 12^+ positive-parity yrast states in ^{80}Kr [band (2)], respectively. The new transitions from the decay of higher-lying states can be seen clearly. Note that the spectrum has been changed by a factor of 3 at 1300 keV γ -ray energy.

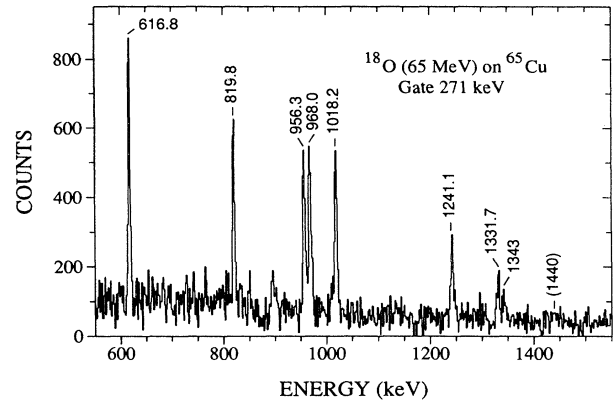


FIG. 2. Gamma-ray spectrum in coincidence with the 271 keV $10_2^+ \rightarrow 10^+$ transition, a linking transition between bands (3) and (2).

of a given peak detected at $35^\circ/145^\circ$ in coincidence with an $E2$ transition detected at 90° by the intensity of the peak detected at 90° in coincidence with the same $E2$ transition detected at $35^\circ/145^\circ$. Based on our detector setup, DCO ratios close to unity and of about 0.5 are predicted for stretched $\Delta I = 2$ and stretched $\Delta I = 1$ transitions, respectively. For most of the strong transitions DCO ratios have been extracted. Whenever possible, the DCO ratios determined from gates on several $E2$ transitions close to the line in question were averaged. Table I presents energy, spin, and parity assignments for states in ^{80}Kr together with energies, relative intensities, and DCO ratios of the γ -ray transitions.

III. CONSTRUCTION OF THE LEVEL SCHEME

The level scheme deduced from the present work is shown in Fig. 4. The states have been grouped partly in bands following earlier suggestions based on $E2$ transition probabilities [6] and based on a comparison with the isotone ^{82}Sr [10]. In order to facilitate the discussion,

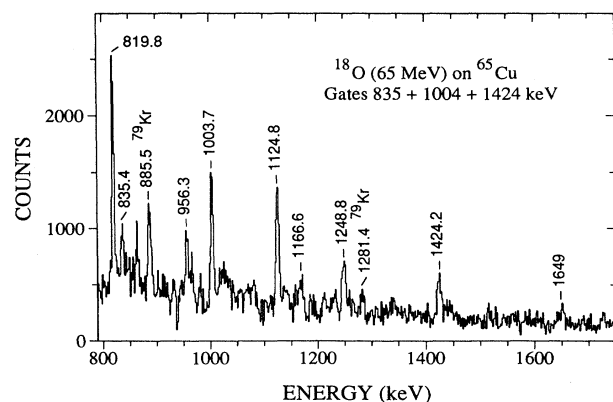


FIG. 3. Sum of spectra in coincidence with the 835, 1004, and 1424 keV transitions of the negative-parity band (5).

TABLE I. Energy, initial and final spins, and parity of levels as well as energy, relative intensity, and DCO ratio for transitions assigned to ^{80}Kr .

E_{lev} (keV)	I_i^π	I_f^π	E_γ (keV)	I_γ^a	R_{DCO}
616.8	2^+	0^+	616.8(2)	100 ^b	1.01(4)
1256.6	2_2^+	2^+	639.8(2)	6(1)	1.04(5)
		0^+	1256.5(3)	2(1)	
1436.6	4^+	2^+	819.8(2)	79(3)	1.03(4)
1788.4	3^+	4^+	351.9(2)	1	
		2_2^+	531.8(2)	4(1)	
		2^+	1171.6(2)	4(1)	
2146.5	4_2^+	4^+	709.9(3)	2(1)	
		2_2^+	889.9(2)	4(1)	
2392.9	6^+	4^+	956.3(2)	71(3)	1.03(4)
2439.5	3^-	2^+	1822.4(7)	1	
2660.3	5^+	3^+	871.7(2)	3(1)	
		4^+	1224.0(4)	1	
2793.6	4^-	3^-	353.7(3)	1	
		4_2^+	647.3(3)	1	
		3^+	1005.1(3)	10(2)	
		4^+	1357.1(4)	2(1)	
2860.3	5^-	3^-	420.3(4)	1	
		4^+	1423.7(3)	11(2)	
3040.7	(5_2^-)	6^+	647.7(3)	1	
		4_2^+	894.2(3)	2(1)	
3042.2	6^-	5^-	182.1(2)	5(1)	1.13(10)
		4^-	248.5(2)	5(1)	1.04(11)
		5^+	381.8(3)	1	
		6^+	649.6(3)	1	
3111.0	6_2^+	6^+	718.1(4)	<1	
		4_2^+	964.5(3)	3(1)	0.9(4)
3173.6	(5_3^-)	5^-	313.3(2)	1	
		6^+	780.7(3)	1	
3346.5	6_2^-	5^-	486.2(3)	1	
		4^-	553(1)	<1	
		5^+	686.2(3)	3(1)	0.57(9)
		6^+	954(1)	1	
3411.1	8^+	6^+	1018.2(2)	58(3)	1.03(4)
3488.7	(6_3^-)	5^-	628.4(3)	1	
		4^-	695.1(4)	1	
		6^+	1096.1(5)	<1	
3531.0	7^-	6_2^+	420.1(3)	1	
		6^-	488.8(2)	6(1)	0.40(10)
		(5_2^-)	490.5(4)	<1	
		6^+	1138.1(3)	1	
3559.4	7_2^-	6^-	517.0(2)	7(1)	0.39(8)
		5^-	699.2(3)	2(1)	
		6^+	1166.6(3)	1	
3582.8	7_3^-	5^-	722.4(3)	4(1)	1.06(9)
		6^+	1190.0(3)	4(1)	0.40(8)
3635.8	7^+	5^+	975.5(4)	1	
3700.9	8_2^+	8^+	289.8(2)	4(1)	1.24(10)
		6^+	1308.3(5)	2(1)	
3917.5	(8_3^+)	8_2^+	216.8(4)	1	
		8^+	507(1)	<1	
		6^+	1524.6(8)	1	
4127.2		7^-	596.1(4)	1	
		6_2^-	780.7(3)	4(1)	
4164.0	(8_2^-)	7_3^-	582(1)	1	
		7^-	632.7(3)	1	
		6^-	1121.8(3)	3(1)	
4379.1	10^+	8_2^+	678.3(3)	1	
		8^+	968.0(2)	40(2)	1.03(4)
4394.7	9^-	7_3^-	811.8(3)	4(1)	1.13(9)

Table I. (Continued).

E_{lev} (keV)	I_i^{π}	I_f^{π}	E_{γ} (keV)	I_{γ}^a	R_{DCO}
4563.6	9_2^-	7_2^-	835.4(3)	7(1)	1.07(14)
		7^-	863.6(3)	5(1)	0.92(14)
		8^+	984.1(4)	1	
		8^-	436.1(4)	<1	
		7_3^-	980.8(3)	4(1)	
4650.1	10_2^+	7^-	1033.0(4)	2(1)	
		8^+	1152.4(4)	1	
		10^+	271.1(2)	3(1)	1.21(13)
		8_2^+	949.4(3)	4(2)	
		8^+	1239.0(4)	6(2)	0.95(11)
4976.5	(10_3^+)	10_2^+	326(1)	<1	
		10^+	597(1)	<1	
		8^+	1565.4(8)	2(1)	0.92(15)
5160.2	(10^-)	8^-	1033.0(3)	4(1)	
5375.4	(10_2^-)	(8_2^-)	1211.4(4)	1	
5398.4	11^-	9^-	1003.7(3)	12(2)	1.01(10)
5439.4	12^+	10^+	1060.3(3)	32(3)	1.05(6)
5666.6	(11_2^-)	(9_2^-)	1103.0(3)	3(1)	
5891.2	12_2^+	12^+	452.0(5)	2(1)	
		10_2^+	1241.1(4)	6(2)	1.07(10)
6182.4	(12^-)	(10^-)	1022.2(4)	1	
6523.2	13^-	11^-	1124.8(4)	7(1)	1.05(10)
6683.0	14^+	12^+	1243.6(4)	20(3)	1.01(10)
7222.9	14_2^+	12_2^+	1331.7(7)	4(1)	0.92(10)
7772.0	15^-	13^-	1248.8(6)	4(1)	1.03(12)
8089.5	16^+	14^+	1406.5(6)	13(3)	1.03(9)
8566	(16_2^+)	14_2^+	1343(1)	4(1)	0.84(17)
9196.2	(17^-)	15^-	1424.2(7)	2(1)	
9692.1	18^+	16^+	1602.6(7)	6(2)	0.99(12)
10845	(19^-)	(17^-)	1649(1)	2(1)	
11485	20^+	18^+	1793(2)	2(1)	1.00(19)

^aIntensities determined from the triangular matrix. Weak lines with one intensity unit only have an uncertainty of about 60%.

^bNormalization.

band numbers have been introduced in Fig. 4 atop the bands similar to the numbers in the ^{82}Sr level scheme.

A. Positive-parity states

The level scheme for the positive-parity yrast band [in Fig. 4 lower part of band (3) connected by the 968 keV transition with band (2)] agrees well with previous work [6,7] through the 14^+ state, and the yrast band has been further extended by three new transitions up to spin 20^+ . The new transitions can be seen in the γ -ray spectrum given in Fig. 1. The highest transition, a weak 1793 keV γ ray in Fig. 1, shows clear coincidences also with the lower-lying transitions at 617, 820, 956, and 1018 keV. The measured DCO ratios confirm the previous spin assignments and suggestions and provide new assignments to all the new states in the yrast band.

Based on our coincidence relations a 949 keV transition has been placed in the band crossing region between the known yrare 10_2^+ and 8_2^+ levels, and the tentative [7] 678 keV $10^+ \rightarrow 8_2^+$ transition has been confirmed. In

addition, some new transitions feeding the 10_2^+ level at 4650 keV have been identified. They can be seen clearly in the 271 keV gated γ -ray spectrum shown in Fig. 2. The strong 1241 keV peak establishes a level at 5891 keV. It is the third transition at about this energy in the level scheme of ^{80}Kr . The known 1239 and 1244 keV transitions depopulating the 10_2^+ and 14^+ states, respectively, cannot account for the observed coincidences. The new level at 5891 keV is supported by a weak 452 keV $12_2^+ \rightarrow 12^+$ decay branch. The next new transition at 1332 keV firmly establishes a level at 7223 keV. A γ ray of this energy was already mentioned in Ref. [6] but not placed. There are some more weak transitions, e.g., at 1343 keV and 1440 keV, which show up in various coincidence gates of the positive-parity sequence; however, no definite placement could be made. It should be mentioned that our 1343 keV line is related to the high-spin sequence. Decay data showed [17] that there might also be a new low-lying transition of this energy in ^{80}Kr .

The low-lying positive-parity sequence 2_2^+ to 6_2^+ is shown below the 8_2^+ state at 3701 keV, i.e., in Fig. 4 below band (2), merely for convenience. No evidence was

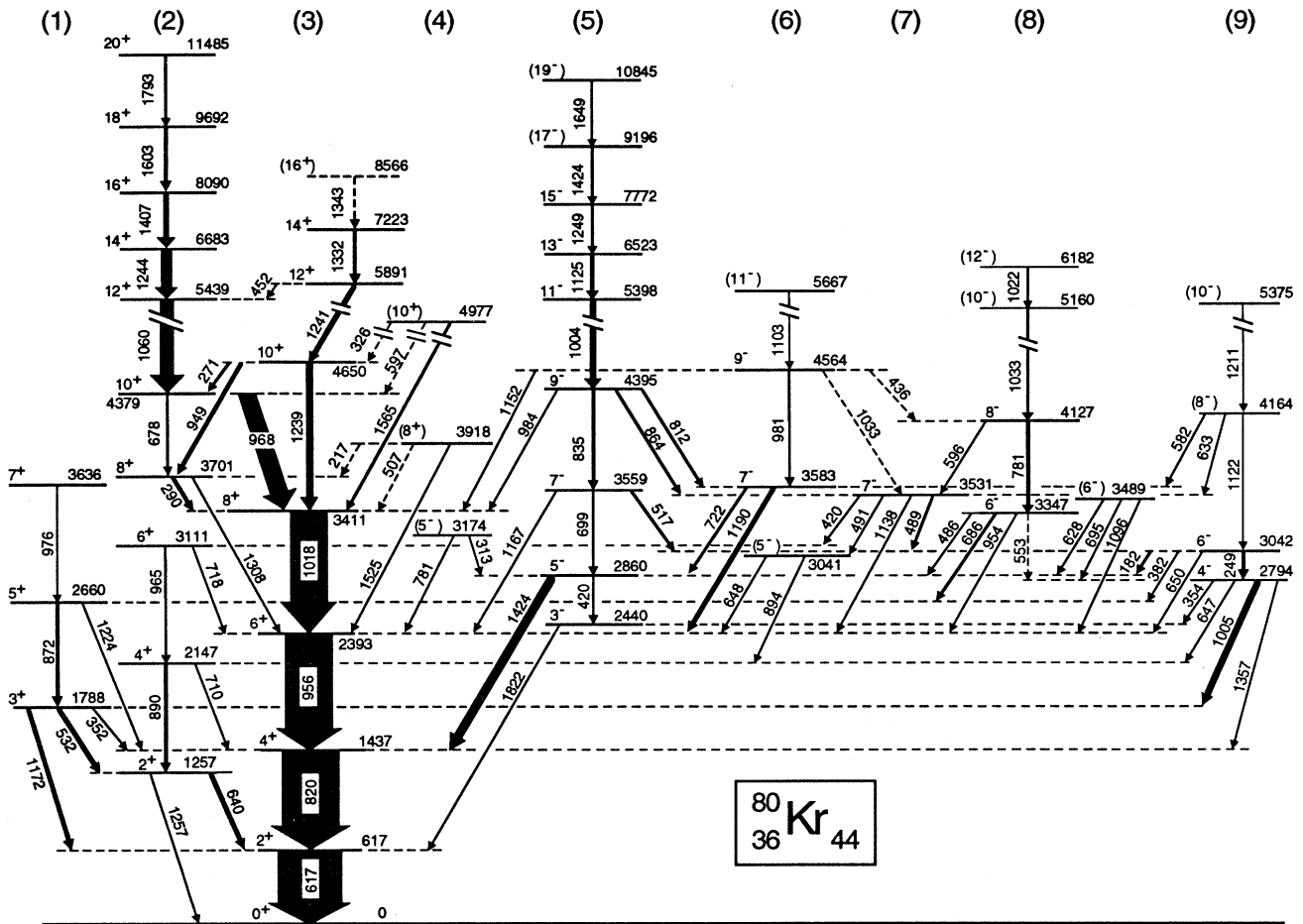


FIG. 4. Level scheme of ^{80}Kr determined in the present work. Some spin and parity assignments for low-lying levels have been adopted from Refs. [6,7].

found for a 590 keV $8_2^+ \rightarrow 6_2^+$ transition which would connect the two decay sequences, e.g., as observed in the isotone ^{82}Sr [9,10] by a 786 keV $E2$ transition. Both the 2_2^+ to 6_2^+ and 3^+ to 7^+ [in Fig. 4 band (1)] sequences in ^{80}Kr were populated weakly in this reaction, and hence it was not always possible to determine DCO ratios for transitions in these bands nor to locate any new states. Therefore, the firm spin and parity assignments given in Fig. 4 were adopted from Refs. [6,7].

B. Negative-parity states

Negative-parity states are known from previous work up to a (10^-) state at 5158 keV [6,7]. Some of them have been placed on top of a 3^- state at 2440 keV due to their $E2$ decays. There are two known 9^- states, at 4395 and 4564 keV, and both have been confirmed in the present work. In addition to the 835 and 864 keV γ -ray transitions to the 7_2^- and 7^- states, respectively, the state at 4395 keV has been found to decay by a new 812 keV transition to the 7_3^- level at 3583 keV and by a 984

keV transition to the 8^+ yrast state. Our DCO ratios of the 812 and 864 keV transitions confirm the previously assigned tentative spin and parity and, in turn, that of the 835 keV decay branch confirms the 7^- assignment for the 3559 keV state.

Since the lowest 9^- state decays with similar strength to each of the 7^- levels, the placement of the three 7^- states into decay sequences is somewhat arbitrary. In previous work [6,7] the highest 7^- state was considered to form a band with the lowest 5^- state due to the observed $E2$ transition strength of 23(5) Weisskopf units (W.u.) for the 722 keV γ ray. However, our coincidence data showed that the highest 7^- state is connected with the onset of another band formed by the 981 keV and the new 1103 keV transitions, [see Fig. 4, band (6)]. Therefore, it seems more appropriate that the weaker 699 keV transition may be a member of band (5). It should be noted that a decay of the third 7^- state to the second or third 5^- states has not been seen.

The lowest 9^- level (at 4395 keV) is populated by five new transitions which extend the decay sequence up to a tentative 19^- level at 10845 keV [see Fig. 4, band (5)].

A relevant background-corrected sum spectrum is given in Fig. 3 where the new transitions can be seen. Two transitions of this new sequence form close-lying doublets with known lower-lying transitions in ^{80}Kr , namely the 1004 and the 1424 keV γ rays. In particular, the interfering $5^- \rightarrow 4^+$ 1424 keV transition and poor statistics prohibit the extraction of reliable DCO ratios for the two uppermost transitions. Therefore, these spins are given tentatively, based on systematics.

The even-spin decay sequence of negative parity [band (8) in Fig. 4] was known [6] up to a (10^-) level at 5160 keV. The previous levels could be confirmed. But only one more transition, an 1022 keV γ ray, leading to a 6182 keV level was added. However, this new transition is smaller in energy than the lower transition, and somewhat unexpected from a comparison with ^{82}Sr . Also, the other sequence of even spins, band (9) in Fig. 4, has been extended by one transition, a 1211 keV γ ray. A 463 keV line has been observed in various coincidence gates of this band, but no definite placement in the level scheme could be made.

A previously observed 313 keV transition [6], so far not placed in the level scheme, has been seen too. Based on our (weak) coincidences a level at 3174 keV is now proposed with a tentative 5^- assignment. This is the third 5^- state; however, no feeding transitions from the higher-lying 7^- states could be identified. In addition, a weak 852 keV γ ray has been found in coincidence with the 1424 keV $5^- \rightarrow 4^+$ and lower-lying transitions, but the placement is uncertain.

A comparison of the low-lying states in ^{80}Kr with those in ^{82}Sr [10] shows a one-to-one correspondence for all states except for a missing second 4^- state in ^{80}Kr which would correspond to the 3007 keV level in ^{82}Sr .

IV. DISCUSSION

Although there are many similar features between the level scheme of ^{80}Kr and that of the nearby even- A Kr isotopes ^{76}Kr [4,13,20], ^{78}Kr [4,13], and ^{82}Kr [3,21,22], its low-spin energy spectrum and high-spin band structure are most similar to that of the isotone ^{82}Sr [9,10]. Both nuclei show a well-pronounced band crossing in the positive-parity yrast band around spin $10\hbar$ and several nonyrast side bands which will be analyzed in more detail below.

A. Cranked-shell-model analysis

1. Band crossings in the positive-parity states

The cranked-shell model can provide further information about the structure of ^{80}Kr and its relation to nearby nuclei. An extensive analysis of quasiparticle excitations around mass $A \approx 80$ has already been presented in Ref. [6], and two-quasiparticle-plus-rotor calculations at prolate deformation have been performed in Ref. [7]. In both papers the conclusion was drawn that in ^{80}Kr at spins $8\hbar$ and $10\hbar$ the positive-parity ground-state band is crossed

by an aligned two-quasiparticle, $g_{9/2}$ proton, band. This conclusion is mainly based on a comparison of experimental aligned angular momenta and on the assumption of similar (prolate) quadrupole deformation which is now questioned. Large $M1$ transition strengths [23] of 1.0(5) and 0.8(4) W.u. for the 271 and 290 keV $\Delta I = 0$ transitions, respectively, do support the interpretation in terms of two crossing bands, although they do not allow a distinction between $g_{9/2}$ proton or neutron alignment.

The kinematic, $J^{(1)}$, moments of inertia for the positive-parity yrast band of ^{80}Kr are shown in Fig. 5 along with those of nearby Kr isotopes. The known backbend in the yrast band of ^{80}Kr at $\hbar\omega \approx 0.50$ MeV was interpreted as a $g_{9/2}$ proton alignment in the previous analysis [6,7], although the present information will bring some doubts into the suggested proton nature of the aligned two quasiparticles. As Fig. 5 shows, the first alignment occurs in ^{78}Kr at $\hbar\omega \approx 0.56$ MeV, a slightly higher frequency than in ^{80}Kr , and at 0.68 MeV in $^{74,76}\text{Kr}$ (the nucleus ^{74}Kr is not shown in Fig. 5). The first crossing in $^{74,76}\text{Kr}$ is connected with a large gain in aligned angular momentum (almost twice that of ^{78}Kr) and was, therefore, interpreted as a simultaneous alignment of $g_{9/2}$ protons and $g_{9/2}$ neutrons [2,13,20]. In ^{78}Kr a second band crossing has been seen at $\hbar\omega \approx 0.9$ MeV pointing to a situation where $g_{9/2}$ protons and $g_{9/2}$ neutrons align at different frequencies. If this trend would persist through ^{80}Kr , the second alignment in the positive-parity yrast band would take place beyond the observed frequency range. However, such a large second crossing frequency ($\hbar\omega > 0.9$ MeV) is difficult to explain in either case, $g_{9/2}$ proton or $g_{9/2}$ neutron alignment.

The band crossing interpretation in ^{80}Kr is somewhat reflected in the way the level scheme has been drawn. It shows that the aligned two-quasiparticle band [band (2)] is built on the second 8^+ state at 3701 keV and becomes yrast through the 10^+ state at 4379 keV. Even though the states in the band crossing region are mutually mixed, as already pointed out in Refs. [6,23], some band assignments have been made based on the predominant decay components. Using these assignments, the kinematic and

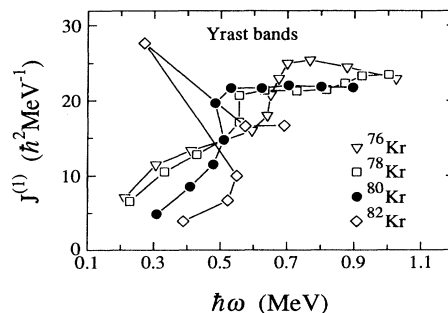


FIG. 5. Kinematic moments of inertia, $J^{(1)}$, for the positive-parity yrast bands in ^{80}Kr and nearby Kr isotopes. A value of $K = 0$ has been used for all bands. The experimental data has been taken from: $^{76,78}\text{Kr}$ Refs. [4,13] and ^{82}Kr Ref. [3].

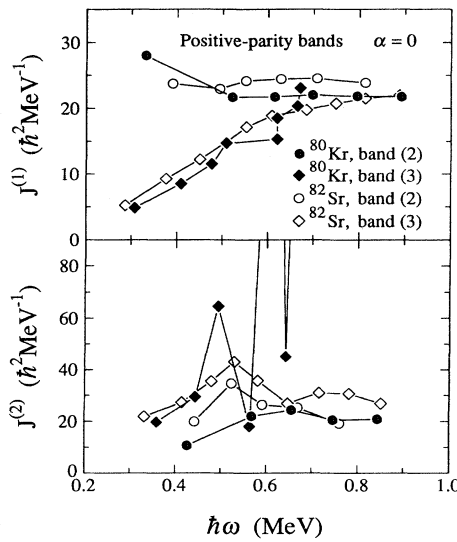


FIG. 6. Kinematic, $J^{(1)}$, and dynamic, $J^{(2)}$, moments of inertia for the positive-parity bands in ^{80}Kr and ^{82}Sr . The ^{82}Sr data and related labels have been taken from Ref. [10] whereas the two uppermost transitions in band (2) of ^{82}Sr have been adopted from Ref. [9]. A value of $K = 0$ has been used for the ground-state bands, bands (3), and $K = 2$ for the $2qp$ excitations, bands (2).

dynamic moments of inertia have been deduced for bands (2) and (3) and plotted as a function of the rotational frequency in Fig. 6. For comparison the moments of inertia for the corresponding bands in ^{82}Sr have been graphed too. The two-quasiparticle band in ^{82}Sr is assumed to be built on the second 8^+ state at 3622 keV and becomes yrast at spin $12\hbar$, a somewhat higher spin than in ^{80}Kr . In both nuclei the bands show a smooth behavior in the kinematic moment of inertia with the ^{80}Kr figures being about 10% lower at high spins. The large displacement at the lowest point of band (2) in ^{80}Kr is due to a stronger interaction with the ground-state band than in ^{82}Sr . In both nuclei the yrast two-quasiparticle bands [bands (2)] do not experience a second band crossing at high spins as can be seen in Fig. 6 from the smooth behavior of the dynamical moments of inertia. In ^{82}Sr this two-quasiparticle yrast band is considered to be oblate deformed [9]. For spins $I > 14\hbar$ an additional smooth alignment of $g_{9/2}$ neutrons is predicted to take place.

In contrast, in both nuclei the extensions of the ground-state bands [bands (3)] through nonyrast states, not seen in any of the lighter even-even Kr isotopes, exhibit fluctuations in the dynamical moments of inertia. These happen at spins of about 12 and 16 in ^{80}Kr and ^{82}Sr , or at rotational frequencies of about $\hbar\omega = 0.62$ and 0.75 MeV, respectively. Therefore, a second crossing is assumed in ^{80}Kr caused by a two-quasiparticle band opposite in nature to the first crossing as already suggested for ^{82}Sr [9].

All experimental crossing frequencies observed in the positive-parity bands of the even-even Kr and Sr nuclei are plotted in Fig. 7 as function of the neutron num-

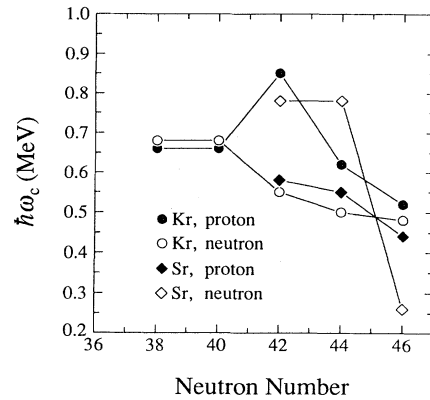


FIG. 7. Experimental proton and neutron crossing frequencies, $\hbar\omega_c$, as a function of the neutron number for some Kr and Sr nuclei. The lines have been drawn to guide the eye. The experimental data has been taken from the positive-parity bands of ^{74}Kr Refs. [1,2], $^{76,78}\text{Kr}$ Refs. [4,13], ^{82}Kr Ref. [3], ^{80}Sr Ref. [24], ^{82}Sr Refs. [9,10], and ^{84}Sr Refs. [25,26].

ber. The comparison and identification of quasiparticle alignments (protons or neutrons) among those Kr isotopes is complicated by predicted shape differences and the strong dependence of crossing frequencies on the quadrupole deformation β_2 and the triaxiality parameter γ [4]. Although a well-deformed prolate shape ($\beta_2 \approx 0.35$) is predicted to be favored for the ground-state band of ^{76}Kr , the nearby nucleus ^{78}Kr is predicted to be very γ soft with competing oblate and triaxial shapes [27–30]. For ^{78}Kr , the alignment of a $g_{9/2}$ proton pair at the first crossing was considered [4] to be the most likely scenario, but doubts were raised because of the two competing shapes and the difficulty of accounting theoretically for the high frequency of the second alignment by $g_{9/2}$ neutrons. A recent discussion [5] of g factors (although no measured g -factor values are given) in the yrast band of ^{78}Kr indicates a $g_{9/2}$ neutron alignment at the first crossing at $\hbar\omega = 0.56$ MeV, which would be consistent with the oblate, rather than the triaxial shape.

Equilibrium calculations for ^{80}Kr (see Sec. IV B.) also favor an oblate shape for the low-lying positive-parity yrast excitations. The calculated quasiparticle energies for this shape are given in Fig. 8 for both protons and neutrons. This leads to the conclusion that a $g_{9/2}$ neutron alignment is predicted to occur first at approximately the observed backbending frequency of $\hbar\omega \approx 0.5$ MeV, while the lowest $g_{9/2}$ proton alignment is calculated at about 0.7 MeV, slightly higher than the observed second crossing. This interpretation, first a $g_{9/2}$ neutron and subsequently a $g_{9/2}$ proton crossing, would be in line with the isotopes ^{78}Kr and ^{82}Kr [3] where in analogy to the measured g factor of the yrast 8^+ state in ^{84}Sr [11,31] the $g_{9/2}$ neutrons were considered to align first.

However, a further complication is that the alignment at the same frequency ($\hbar\omega = 0.55$ MeV) in the $N = 44$ isotones ^{84}Zr and ^{82}Sr has been identified unambiguously with $g_{9/2}$ protons from g -factor measurements [8,11].

The question of which particles align first in these nu-

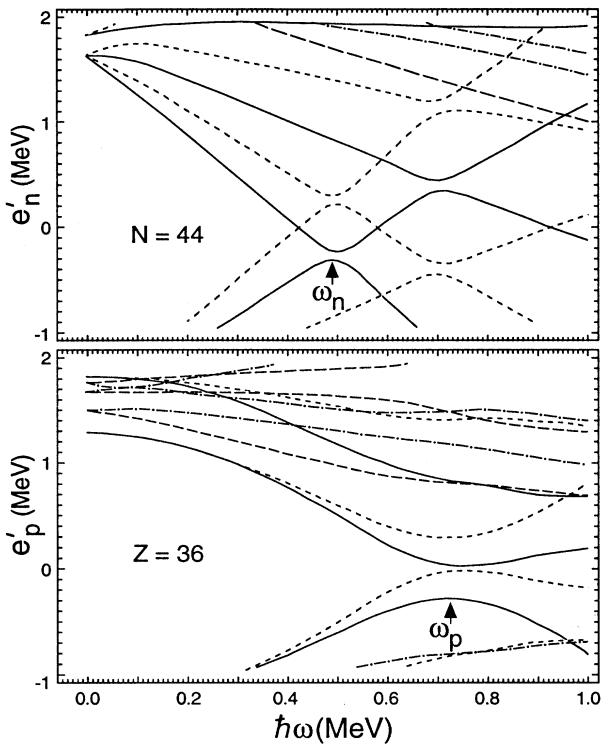


FIG. 8. Proton and neutron quasiparticle Routhians calculated for ^{80}Kr with a fixed shape of $\beta_2 = 0.245$, $\gamma = -53.6^\circ$, and $\beta_4 = -0.012$. Parity and signature of the Routhians are indicated in the following way: $(\pi = +, \alpha = \frac{1}{2})$, solid line; $(\pi = +, \alpha = -\frac{1}{2})$ dotted line; $(\pi = -, \alpha = \frac{1}{2})$ dash-dotted; $(\pi = -, \alpha = -\frac{1}{2})$ dashed line. Crossing frequencies of $\hbar\omega_c = 0.73$ and 0.5 MeV have been deduced for $g_{9/2}$ protons and $g_{9/2}$ neutrons, respectively.

clei is closely coupled to that of their shapes, which are very sensitive to many influences and may change dramatically from nucleus to nucleus, or even from band to band [32]. As a result, comparisons between nearby nuclei have to be treated with caution. Since the shapes predicted by the Hartree-Fock-Bogolyubov (HFBC) calculations have often been verified at least qualitatively, it seems more likely at this time that the yrast band of ^{80}Kr is associated with a near-oblate shape and that the band crossing at $\hbar\omega \approx 0.5$ MeV is due to a $g_{9/2}$ neutron alignment, in apparent analogy with ^{78}Kr and ^{82}Kr , but opposite to the case of ^{82}Sr or ^{84}Zr . Clearly a measurement of g factors in the region of the first alignment in ^{80}Kr could help to bring more evidence into this matter.

2. Negative-parity bands

The negative-parity sequences in $^{76,78}\text{Kr}$ show an almost constant kinematic moment of inertia and are considered as one of the best examples of collective rotation in the mass 80 region. For ^{80}Kr , however, such a well-developed high-spin band was not known prior to this work. Attempts have been made to interpret the low-

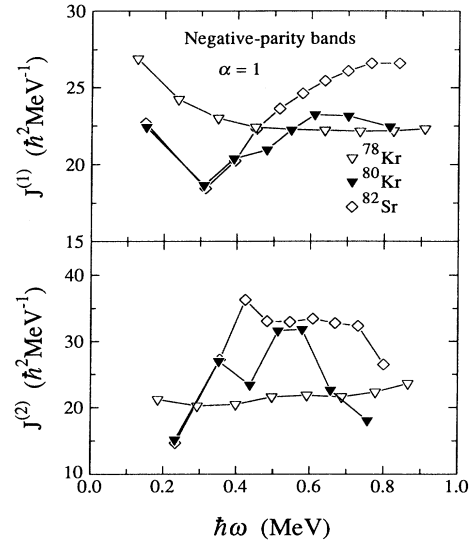


FIG. 9. Kinematic, $J^{(1)}$, and dynamic, $J^{(2)}$, moments of inertia for negative-parity bands with signature $\alpha = 1$ in ^{80}Kr [band (5)] and neighboring even-even nuclei. In the analysis a value of $K = 3$ has been used for all bands.

lying states using the cranked-shell model [6,7] and the interacting boson model [33].

Based on a cranked-shell-model analysis of the aligned angular momenta of the negative-parity bands in ^{80}Kr at low rotational frequency, a $g_{9/2}$ proton structure combined with a 3^- octupole excitation has been proposed [6]. In the lighter isotopes $^{76,78}\text{Kr}$ [4] a similar conclusion about the negative-parity bands was deduced. The observed extensions of the bands in ^{80}Kr and their resemblance to the neighbors support this assignment.

The kinematic, $J^{(1)}$, and dynamic, $J^{(2)}$, moments of inertia for the negative-parity bands with signature $\alpha = 1$ in ^{78}Kr , ^{80}Kr [band (5)], and ^{82}Sr [band (5) in Ref. [10]] are compared in Fig. 9. It can be seen that the $J^{(1)}$ moments of inertia in ^{80}Kr below 0.4 MeV rotational frequency are close to those of ^{82}Sr . With increasing frequency the behavior deviates more and more from ^{82}Sr and comes closer to ^{78}Kr . The peak in the $J^{(2)}$ moments at $\hbar\omega \approx 0.55$ MeV may indicate a band crossing which has been seen in ^{82}Sr , but not in ^{78}Kr . Blocking arguments favor the alignment of a $g_{9/2}$ neutron pair, in agreement with the crossing frequency deduced for neutrons. The alignment leads to a four-quasiparticle structure for the band at spins higher than 13^- . This interpretation is in line with the findings for band (5) in ^{82}Sr where the observed broad peak has been related to a $g_{9/2}$ neutron alignment [9] too.

The second band of negative parity with $\alpha = 1$ in ^{80}Kr , band (6), may start with the third 7^- state at 3583 keV. A decay to the second 5^- state at 3041 keV, analogous to that in ^{82}Sr , has not been observed. The moments of inertia (not shown) are increasing somewhat, but the band is too short to draw definite conclusions.

The $J^{(1)}$ and $J^{(2)}$ moments of inertia for the negative-parity bands with signature $\alpha = 0$, band (8), are given in

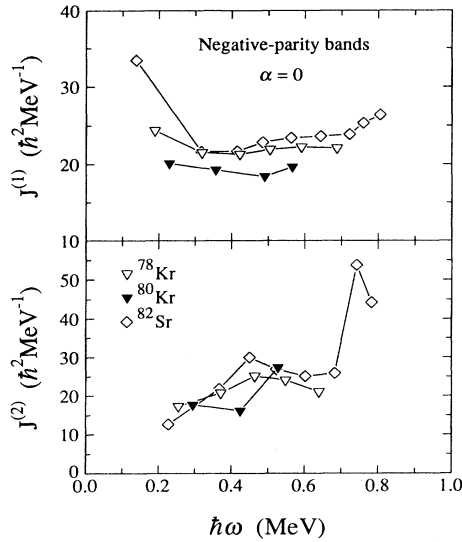


FIG. 10. Kinematic, $J^{(1)}$, and dynamic, $J^{(2)}$, moments of inertia for negative-parity bands with signature $\alpha = 0$ in ^{80}Kr [band (8)] and neighboring even-even nuclei. In the analysis a value of $K = 3$ has been used for all bands.

Fig. 10 along with the data for some neighbors. Again, a $g_{9/2}$ proton structure has been suggested previously [6,7] for this band in ^{80}Kr , and for the corresponding bands in $^{76,78}\text{Kr}$ [4] and ^{82}Sr [9]. The similarities in the smooth behavior of the $J^{(1)}$ moments of inertia support the common configuration, even though the ^{80}Kr moments are slightly lower. The sharp peak in $J^{(2)}$ for ^{82}Sr [band (8)] at about 0.75 MeV rotational frequency has been attributed to an additional $g_{9/2}$ proton alignment [9] not seen in $^{78,80}\text{Kr}$.

B. Shape changes in ^{80}Kr

As discussed above, the interpretation of the observed quasiparticle alignments in ^{80}Kr and the comparison with its neighbors depend sensitively on the underlying shape, whether prolate, oblate, or triaxial. Calculations of the potential-energy surface and nuclear ground-state deformation for the even-even Kr isotopes have previously been performed using a Yukawa-plus-exponential macroscopic model [27,28]. For ^{80}Kr (see Fig. 31 in Ref. [28]) a quite flat energy surface was obtained with the prolate minimum slightly deeper than the oblate one. For the prolate minimum an electric quadrupole moment of 0.7 eb [27] has been calculated, which would correspond to an axial deformation of $\beta_2 = 0.09$. Similar results have been obtained from theoretical equilibrium deformations calculated within the configuration-dependent shell-correction approach (Hartree-Fock-Bogolyubov cranking model with a Woods-Saxon potential) [29] for ^{80}Kr which also show an almost flat ground-state energy surface for $|\beta_2| \leq 0.3$ when pairing is included, with two minima only 50 keV

apart; an oblate minimum at $\beta_2 = -0.20$ and a prolate minimum at $\beta_2 = 0.10$ (see Table 1 of Ref. [29]). Without pairing a large oblate ground-state deformation is favored due to the oblate $Z = 36$ gap in the single-particle energies. The flatness of the energy surface for the ground state implies that a small amount of rotational energy might be sufficient to drive the nucleus towards the more deformed oblate shape. Two examples of the total Routhian surfaces (TRS) calculated for ^{80}Kr within the Hartree-Fock-Bogolyubov cranking model [29] at different rotational frequencies are shown in Figs. 11(a) and (b) for the vacuum configuration, which represents the ground-state band. The minimum in the plot for $\hbar\omega = 0.30$ MeV (representing a situation below the band crossing) describes a near-oblate shape with $\beta_2 = 0.24$, $\gamma = -53.6^\circ$, and $\beta_4 = -0.012$. This is the shape which implies that the $g_{9/2}$ neutrons align at a lower frequency than the $g_{9/2}$ protons. However, the shape is quite soft both in the γ direction and towards smaller β_2 values. Above the band crossing at $\hbar\omega = 0.59$ MeV essentially the same shape remains favored but with much less softness towards smaller deformations. According to the calculations the excitation of the $g_{9/2}$ neutrons is shortly followed by a gradual alignment of a $g_{9/2}$ proton pair. This leads to a four-quasiparticle configuration for spins $I > 14\hbar$ which forms the positive-parity yrast sequence as in ^{82}Sr .

It should be noted that the calculations also provide a well-deformed near-prolate band of positive-parity which lies an average of only 400 keV above the lowest near-oblate yrast band. This band is connected with the first alignment of a $g_{9/2}$ proton pair. The theoretical evolution predictions of the different shapes for the positive-parity states are shown in Fig. 12 in a polar coordinate diagram.

The lifetimes reported in Ref. [6] provide experimental information on the quadrupole deformation of ^{80}Kr . The deduced average transition quadrupole moment $|Q_t|$ in the ground-state band is 2.0(3) eb, corresponding to an axial quadrupole deformation of $|\beta_2| = 0.25(3)$. This is in good agreement with the predicted magnitude of the deformation from Fig. 11, but provides no direct information about the γ degree of freedom.

The Hartree-Fock-Bogolyubov cranking model calculations [29] also predict that for spins of $I \geq 20\hbar$, first a well-deformed and subsequently a strongly deformed near-prolate band will become yrast, as can be seen in Fig. 11 (c). The strongly deformed band is predicted to contain the lowest $h_{11/2}$ neutron orbital. The prediction of this superdeformed band is very similar to the corresponding band in ^{82}Sr . However, this spin region is far beyond the present experimental results.

For the negative-parity bands there is a larger variation among the $|Q_t|$ values inferred from the measured lifetimes. The average value is 1.7(8) eb with a large standard deviation which would imply an axial deformation of 0.22(10). In general, the negative-parity states are considered to consist of a two-proton configuration which may be represented by the configuration fa in Fig. 11 (d). Two minima can be seen in the theoretical TRS plot. The absolute minimum in the prolate noncollective sector would imply a $|Q_t|$ value of 0.9 eb, while the

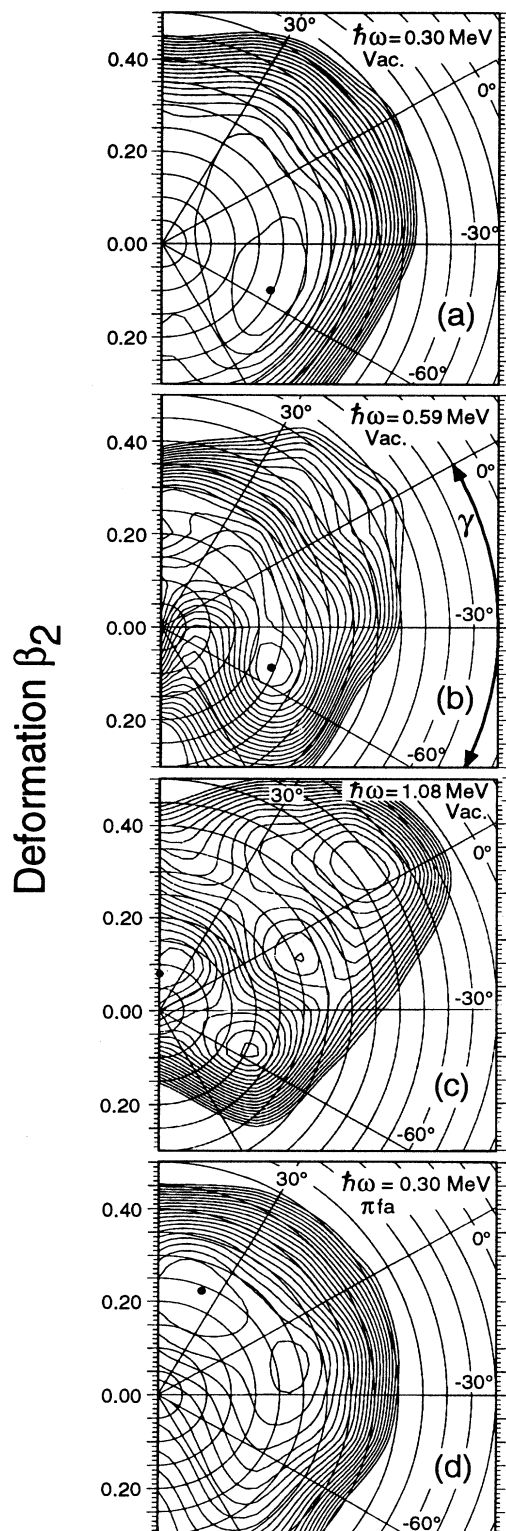


FIG. 11. Total Routhian surfaces in the (β_2, γ) plane calculated using the Hartree-Fock-Bogolyubov cranking model with a Woods-Saxon potential for rotational frequencies of $\hbar\omega = 0.30$ and 0.59 MeV [29]. Graphs (a), (b), and (c) are calculated for the positive-parity vacuum configuration, and graph (d) for a two-quasiproton (fa) configuration leading to negative parity and signature $\alpha = 1$.

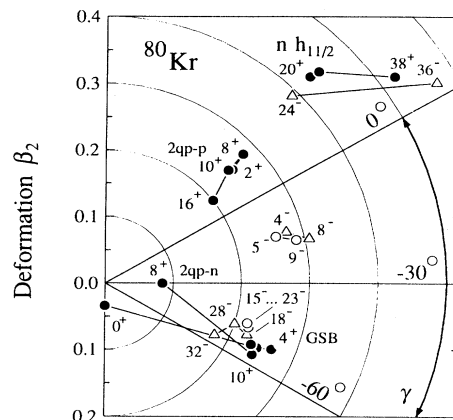


FIG. 12. Calculated equilibrium deformations in the (β_2, γ) plane for different configurations in ^{80}Kr . The symbols follow: GSB, ground-state band; $2qp-p$, two-quasiparticle excitation with predominating $g_{9/2}$ protons; $2qp-n$, two-quasiparticle excitation with predominating $g_{9/2}$ neutrons.

somewhat higher collective triaxial minimum would give about 2.8 eb, about 60% larger than the average experimental value. These triaxial minima have been assigned to the low-spin negative-parity states plotted in Fig. 12. Since the transition quadrupole moments were only measured for states of spin 5^- to 8^- in the region of strong mixing, the mixed nature of these states may lower the $E2$ transition strengths. Therefore, it is quite possible that the collective triaxial shape with $\beta_2 \approx 0.27$ and $\gamma \approx -18^\circ$ may represent the low-lying negative-parity states. For higher states of negative parity ($I > 9\hbar$), a near-oblate shape but with less quadrupole deformation is predicted for both signatures. At spins around 24^- a competing well-deformed near-prolate band might be populated which would drive the nucleus towards a strongly deformed prolate shape.

V. SUMMARY

High-spin states in ^{80}Kr were populated using the $^{65}\text{Cu}(^{18}\text{O}, p2n)$ reaction at 65 MeV. Prompt γ - γ coincidences were measured using the Pitt-FSU detector array with nine Compton-suppressed Ge detectors and a 28-element BGO multiplicity filter. The positive-parity yrast band was extended by three new transitions up to the 20^+ state. The kinematic and dynamic moments of inertia of the new high-spin members of the yrast band remain quite constant at about $21 \hbar^2/\text{MeV}$ and show no obvious evidence of a second band crossing for $\hbar\omega < 0.9$ MeV. However, the extension of the ground-state band through nonyrast states shows a band crossing at $\hbar\omega \approx 0.62$ MeV which may be caused by a two-quasiparticle band opposite in nature to the band at the first crossing.

A question remains about the identity of the particles which align first in the positive-parity yrast band

at $\hbar\omega \approx 0.5$ MeV. A $g_{9/2}$ proton alignment was originally suggested based on a comparison of the amount of aligned angular momentum in neighboring odd- A nuclei. However, the theoretically predicted near-oblate shape would imply a $g_{9/2}$ neutron alignment at this frequency. Systematics of experimental data from $Z = 36$ nuclei support that the $g_{9/2}$ neutrons align first, but those from $N = 44$ nuclei favor $g_{9/2}$ protons. A measurement of the g factors just above the first band crossing would best resolve this question in ^{80}Kr . The magnitude of the theoretically predicted oblate deformation is consistent with the previously measured lifetimes, but this does not directly prove that the shape is oblate.

A new negative-parity high-spin band was found above the 4395 keV 9^- level, and the onset of an additional decay sequence built on the second 9^- state has been observed. The high degree of mixing seen among the medium-spin negative-parity states is similar to that of

the isotope ^{82}Sr and may be partly due to admixtures with an octupole phonon. As in ^{82}Sr a negative-parity band with no signs of mixing has been found above a 9^- state. All in all, a very close resemblance is seen between the negative-parity structures of the isotones ^{80}Kr and ^{82}Sr .

ACKNOWLEDGMENTS

We are grateful to Dr. J.X. Saladin, whose loan of the University of Pittsburgh detectors and electronics made the combined Pitt-FSU detector array possible. We wish to thank Dr. W. Nazarewicz for providing computer codes for calculating quasiparticle Routhians and for results of his HFB total Routhian surfaces calculations. This work was supported in part by the National Science Foundation.

-
- [1] S.L. Tabor, P.D. Cottle, J.W. Holcomb, T.D. Johnson, P.C. Womble, S.G. Buccino, and F.E. Durham, *Phys. Rev. C* **41**, 2658 (1990).
 - [2] J. Heese, D.J. Blumenthal, A.A. Chishti, P. Chowdhury, B. Crowell, P.J. Ennis, C.J. Lister, and Ch. Winter, *Phys. Rev. C* **43**, R921 (1991).
 - [3] P. Kemnitz, P. Ojeda, J. Döring, L. Funke, L.K. Kostov, H. Rotter, E. Will, and G. Winter, *Nucl. Phys.* **A425**, 493 (1985).
 - [4] C.J. Gross, J. Heese, K.P. Lieb, S. Ulbig, W. Nazarewicz, C.J. Lister, B.J. Varley, J. Billowes, A.A. Chishti, J.H. McNeill, and W. Gelletly, *Nucl. Phys.* **A501**, 367 (1989).
 - [5] J. Billowes, F. Cristancho, H. Grawe, C.J. Gross, J. Heese, A.W. Mountford, and M. Weiszflog, *Phys. Rev. C* **47**, R917 (1993).
 - [6] L. Funke, J. Döring, F. Dubbers, P. Kemnitz, E. Will, G. Winter, V.G. Kiptilij, M.F. Kudojarov, I.Kh. Lemberg, A.A. Pasternak, A.S. Mishin, L. Hildingsson, A. Johnson, and Th. Lindblad, *Nucl. Phys.* **A355**, 228 (1981).
 - [7] D.L. Sastry, A. Ahmed, A.V. Ramayya, R.B. Piercey, H. Kawakami, R. Soundranayagam, J.H. Hamilton, C.F. Maguire, A.P. de Lima, S. Ramavataram, R.L. Robinson, H.J. Kim, and J.C. Wells, *Phys. Rev. C* **23**, 2086 (1981).
 - [8] A.W. Mountford, J. Billowes, W. Gelletly, H.G. Price, and D.D. Warner, *Phys. Lett. B* **279**, 228 (1992).
 - [9] C. Baktash, G. Garcia-Bermudez, D.G. Sarantites, W. Nazarewicz, V. Abenante, J.R. Beene, H.C. Griffin, M.L. Halbert, D.C. Hensley, N.R. Johnson, I.Y. Lee, F.K. McGowan, M.A. Riley, D.W. Stracener, T.M. Semkow, and A. Virtanen, *Phys. Lett. B* **255**, 174 (1991).
 - [10] S.L. Tabor, J. Döring, J.W. Holcomb, G.D. Johns, T.D. Johnson, T.J. Petters, M.A. Riley, and P.C. Womble, *Phys. Rev. C* **49**, 730 (1994).
 - [11] A.I. Kucharska, J. Billowes, and C.J. Lister, *J. Phys. G* **15**, 1039 (1989).
 - [12] R. Schwengner, G. Winter, J. Döring, L. Funke, P. Kemnitz, E. Will, A.E. Sobov, A.D. Efimov, M.F. Kudojarov, I.Kh. Lemberg, A.S. Mishin, A.A. Pasternak, L.A. Ras-sadin, and I.N. Chugunov, *Z. Phys. A* **326**, 287 (1987).
 - [13] M.S. Kaplan, J.X. Saladin, L. Faro, D.F. Winchell, H. Takai, and C.N. Knott, *Phys. Lett. B* **215**, 251 (1988).
 - [14] D.G. McCauley and J.E. Draper, *Phys. Rev. C* **4**, 475 (1971).
 - [15] H.-G. Friederichs, A. Gelberg, B. Heits, K.P. Lieb, M. Uhrmacher, K.O. Zell, and P. von Brentano, *Phys. Rev. Lett.* **34**, 745 (1975).
 - [16] N. Yoshikawa, Y. Shida, O. Hashimoto, M. Sakai, and T. Numao, *Nucl. Phys.* **A327**, 477 (1979).
 - [17] A. Giannatiempo, A. Nannini, A. Perego, P. Sona, M.J.G. Borge, K. Riisager, O. Tengblad, and ISOLDE Collaboration, *Phys. Rev. C* **47**, 521 (1993).
 - [18] S.L. Tabor, M.A. Riley, J. Döring, P.D. Cottle, R. Books, T. Glasmacher, J.W. Holcomb, J. Hutchins, G.D. Johns, T.D. Johnson, T. Petters, O. Tekyi-Mensah, P.C. Womble, L. Wright, and J.X. Saladin, *Proceedings of the Twelfth International Conference on the Application of Accelerators in Research and Industry*, Denton, Texas, 1992 [*Nucl. Instrum. Methods Phys. Res. Sect. B* **79**, 821 (1993)].
 - [19] S.L. Tabor, *Nucl. Instrum. Methods Phys. Res. Sect. A* **265**, 495 (1988).
 - [20] C.J. Gross, J. Heese, K.P. Lieb, L. Lühmann, B. Wörmann, A.A. Chishti, W. Gelletly, C.J. Lister, J.H. McNeill, and B.J. Varley, *Z. Phys. A* **331**, 361 (1988).
 - [21] S. Brüssermann, J. Keinonen, H.P. Hellmeister, and K.P. Lieb, *Z. Phys. A* **304**, 335 (1982).
 - [22] S. Brüssermann, K.P. Lieb, P. Sona, H. Emling, E. Grosse, and J. Stachel, *Phys. Rev. C* **32**, 1521 (1985).
 - [23] P. Kemnitz, J. Döring, L. Funke, E. Will, and G. Winter, *Phys. Lett.* **125B**, 119 (1983).
 - [24] R.F. Davie, D. Sinclair, S.S.L. Ooi, N. Poffé, A.E. Smith, H.G. Price, C.J. Lister, B.J. Varley, and I.F. Wright, *Nucl. Phys.* **A463**, 683 (1987).
 - [25] A. Dewald, U. Kaup, W. Gast, A. Gelberg, H.-W. Schuh, K.O. Zell, and P. von Brentano, *Phys. Rev. C* **25**, 226 (1982).
 - [26] S. Chattopadhyay, H.C. Jain, M.L. Jhingan, and C.R. Praharaj, *Phys. Rev. C* **50**, 93 (1994).

- [27] P. Möller and J.R. Nix, *Atomic Data Nucl. Data Tables* **26**, 165 (1981).
- [28] R. Bengtsson, P. Möller, J.R. Nix, and J. Zhang, *Phys. Scr.* **29**, 402 (1984).
- [29] W. Nazarewicz, J. Dudek, R. Bengtsson, T. Bengtsson, and I. Ragnarsson, *Nucl. Phys.* **A435**, 397 (1985).
- [30] D. Galeriu, D. Bucurescu, and M. Ivascu, *J. Phys. G* **12**, 329 (1986).
- [31] C. Broude, E. Dafni, A. Gelberg, M.B. Goldberg, G. Goldring, M. Hass, O.C. Kistner, and A. Zemel, *Phys. Lett.* **105B**, 119 (1981).
- [32] E.F. Moore, P.D. Cottle, C.J. Gross, D.M. Headly, U.J. Hüttmeier, S.L. Tabor, and W. Nazarewicz, *Phys. Lett. B* **211**, 14 (1988); *Phys. Rev. C* **38**, 696 (1988).
- [33] D.N. Dojnikov, A.D. Efimov, K.I. Erokhina, and V.M. Mikhajlov, *Nucl. Phys.* **A531**, 326 (1991).